Chinese Chemical Letters 34 (2023) 108321

Contents lists available at ScienceDirect

Chinese Chemical Letters

journal homepage: www.elsevier.com/locate/cclet

A near-infrared fluorescent probe for fast and precise imaging of senescent cells and ovarian cancer cells *via* tracking β-galactosidase

Haiting Pan[a], Xianzhi Chai[b,*], Junji Zhang[a,*]

[a] Key Laboratory for Advanced Materials and Joint International Research Laboratory of Precision Chemistry and Molecular Engineering, Feringa Nobel Prize Scientist Joint Research Center, School of Chemistry and Molecular Engineering, Frontiers Center for Materiobiology and Dynamic Chemistry, East China University of Science and Technology, Shanghai 200237, China
[b] School of Environmental and Chemical Engineering, Jiangsu University of Science and Technology, Zhenjiang 212100, China

ARTICLE INFO

Article history:
Received 21 December 2022
Revised 1 March 2023
Accepted 8 March 2023
Available online 11 March 2023

Keywords:
β-Galactosidase
Near-infrared fluorescent probe
Senescent cell
Precise imaging
Fast response

ABSTRACT

Aging-related diseases are gradually becoming a major problem with the rapid development of aged population in human society. Although many fluorescent probes have been employed to diagnosis senescence *via* imaging senescence-associated β-galactosidase (SA-β-Gal), which is proved to be closely associated with senescent cells, the similar catalytic effectiveness of enzymatic reaction of ovarian cancer-associated β-Gal (OA-β-Gal) will interfere with imaging accuracy. Herein, a near-infrared (NIR) hemicyanine based fluorescent probe **HCyXA-βGal** was designed for light-up imaging of live cells containing β-Gal. With the organelle-targeting morpholinyl and positive charge moieties, **HCyXA-βGal** was successfully applicated to image the difference of enzymatic location in senescent cells and ovarian cancer cells. Furthermore, inspired by the fast response performance, fast and precise imaging of the two cell lines was realized *via* covering another dimension of fluorescence signal: time-dependent intensity.

Accurate early diagnosis of pathological processes is of great significance in improving therapeutic effect [1]. Biomarkers are the special signaling molecule for identifying diseases, which are produced and released from cells during pathological processes [2]. Hence, monitoring the abnormal content and activity of biomarkers is crucial for diagnosis and therapy. Among various of biomarkers, enzymes possess the abilities to catalyze a certain type of reactions, making them the ideal targets with specificity and sensibility [3]. β-Galactosidase (β-Gal) is a glycoside hydrolase enzyme that catalyses the hydrolysis of β-galactosides into monosaccharides [4,5]. In recent years, senescence-associated β-Gal (SA-β-Gal) has attracted considerable attentions in many researches as a significant biomarker overexpressed in senescent cells [6,7]. The progressive accumulation of senescent cells, once present in sufficient amounts, may actively drive the tissues to be at risk of aging-related diseases, including Alzheimer disease, atherosclerosis, osteoarthritis, cancer, idiopathic pulmonary fibrosis and chronic obstructive pulmonary disease (COPD) [6,8]. Therefore, it is of great value to develop a fast and accurate method for detection of SA-β-Gal activity, desired for understanding and improving preventive interventions for age-related diseases.

Many traditional detection technologies, such as magnetic resonance imaging (MRI), positron emission tomography (PET) and computed tomography (CT), are constrained by the drawbacks of long scanning and post-processing time [9–11]. By contrast, fluorescent probes have received much attention to be a powerful approach for tracing various analytes, taking advantages of high sensitivity, low cost and real-time detection [12–14]. Several fluorescent probes have been successfully applied for the visualization of SA-β-Gal with fast response and improved precision *in vitro* and *in vivo* based on the enzymatic catalytic reaction [15–19]. In addition, ovarian cancer-associated β-Gal (OA-β-Gal) shows the similar catalytic effectiveness of enzymatic reaction comparing with SA-β-Gal and was one of the important biomarkers for ovarian cancer [20–24]. Therefore, the design of fluorescent probes for β-Gal will help researchers diagnose not only cell senescence but also ovarian cancer. Recently, Guo *et al.* [25] reported a two-dimensional fluorescent probe for the precise tracking of cell senescence and ovarian cancer cells by monitoring β-Gal and lysosomal pH simultaneously. This elegant probe achieved precise imaging of senescent cells relying on the unique de-acidification feature of lysosomes in senescent cells. Our group [26] developed a photochromic fluorescent probe for precise imaging of senescent cells and ovar-

* Corresponding authors.
E-mail addresses: chaixianzhi@163.com (X. Chai), zhangjunji@ecust.edu.cn (J. Zhang).

https://doi.org/10.1016/j.cclet.2023.108321
1001-8417/

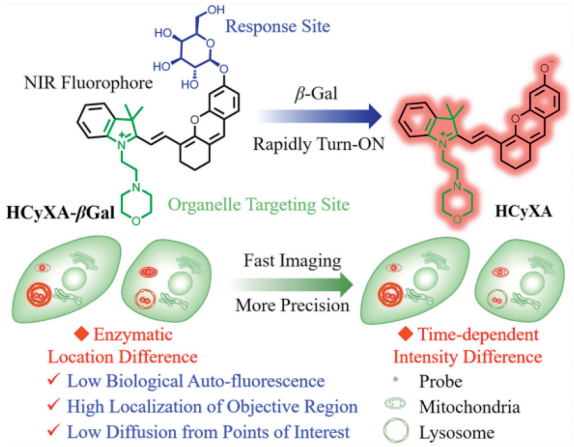

Scheme 1. Design and performing mechanism of probe **HCyXA-*β*Gal** for precise imaging of senescent cells and ovarian cancer cells *via* fast imaging of β-Gal.

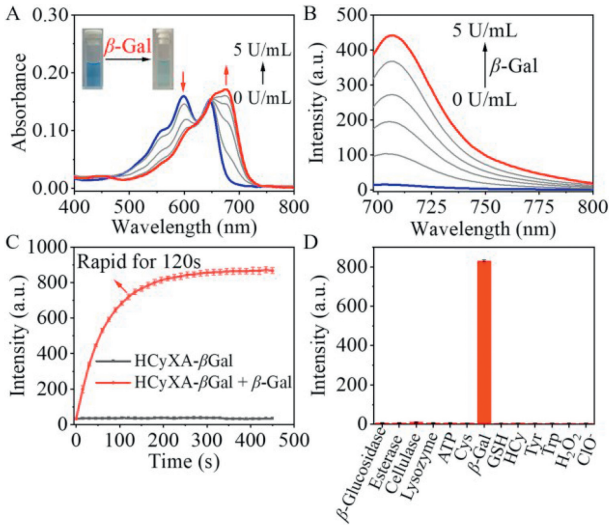

Fig. 1. Spectral profiles of **HCyXA-*β*Gal** incubated with β-Gal in mixed solution (PBS/DMSO = 9:1, v/v, PBS 10 mmol/L, pH 7.4, 37 °C). (A) UV–vis absorption spectra and (B) Emission spectra of **HCyXA-*β*Gal** (10 μmol/L) before and after incubation with different concentrations of β-Gal (0–5 U/mL) for 2 min. Inset: images before and after treatment with β-Gal. (C) Time dependence of emission intensity at 710 nm for **HCyXA-*β*Gal** (10 μmol/L) after incubation with β-Gal (10 U/mL). (D) Emission intensity of at 710 nm of **HCyXA-*β*Gal** (10 μmol/L) upon addition of various species: esterase (10 U/mL), cellulase (10 U/mL), lysozyme (10 U/mL), ATP (100 μmol/L), Cys (100 μmol/L), β-Gal (10 U/mL), GSH (100 μmol/L), HCy (100 μmol/L), Tyr (100 μmol/L), Trp (100 μmol/L), H_2O_2 (100 μmol/L), ClO^- (100 μmol/L) incubation with 20 min. All emissions were produced upon excitation at 680 nm.

ian cancer cells by introducing two dimensions of fluorescence signals for β-Gal: fluorescence-ON and fluorescence-blinking. This blinking probe successfully reached a much improved resolution of *ca.* 80 nm to differentiate the enzymatic distributions in senescent cells (lysosome located) and ovarian cancer cells (random in cytoplasm and organelles), by using stochastic optical reconstruction microscopy (STORM).

Despite the progress in the multi-dimensional imaging of cell senescence, the majority of probe systems developed require more than one channel or costly high resolution imaging science experiment (HIRISE), which are inconvenient and time-consuming. As a result, the development of economical fluorescent probe with easy operation is still a challenging task. Herein, we report a light-up near-infrared (NIR) fluorescent probe **HCyXA-*β*Gal** for fast and precise imaging of senescent cells and ovarian cancer cells *via* tracking β-Gal. The organelle-targeted ability of probe achieved fluorescence imaging difference of enzymatic location in the two cell lines containing β-Gal. The property of rapid response enlightened us to delve into more precise imaging of live cells containing β-Gal *via* covering another dimension of fluorescence signal: time-dependent intensity (Scheme 1). Considering the different location of β-Gal in senescent cells and ovarian cancer cells, the probe is equipped with the lysosome-targeting morpholinyl group and mitochondria-targeting positive charge hemicyanine moiety. Based on the enzymatic catalytic reaction, β-galactoside is introduced at the site of hydroxyl to quench the fluorescence through blocking intramolecular charge transfer (ICT). **HCyXA-*β*Gal** exhibits weak fluorescence in the initial state, while emits bright NIR fluorescence after incubation with β-Gal in solution, with fast response speed. Through its fast response speed that would dramatically shorten imaging time, the diffusion problem of enzyme-activated fluorophores from points of interest (POI) could be alleviated [27,28]. In addition, the NIR emission properties and organelle-targeting ability of **HCyXA-*β*Gal** also facilitate the realization of precise imaging in targeted cells by reducing biological auto-fluorescence and improving capability of localization. Combining the advantages mentioned above, **HCyXA-*β*Gal** has great potential to achieve precise imaging of senescent cells and ovarian cancer cells *via* fast time-lapse imaging to observe enzymatic location status and time-dependent intensity of β-Gal.

HCyXA-*β*Gal was synthesized by Knoevenagel condensation reaction between 2,3,3-trimethyl-3*H*-indole-functionalized morphine and xanthene derivative that was modified with an acetyl-protected β-galactose group on the phenol unit. The subsequent deprotection of the acetate groups afforded the final product **HCyXA-*β*Gal** (Scheme S1 in Supporting information). In addition, **HCyXA** was synthesized (Scheme S1) for use as a control compound in subsequent experiments. With the probe **HCyXA-*β*Gal** in hand, the optical response of probe (10 μmol/L) toward β-Gal was first measured in a mixture of phosphate-buffered saline/dimethyl sulfoxide (PBS/DMSO; v/v = 9:1) in the presence of different concentrations of β-Gal. Upon treatment of β-Gal (0–5 U/mL) for 2 min, the absorbance at 600 nm decreased obviously and a new peak at 685 nm appeared, along with the color changed from blue to cyan (Fig. 1A). Meanwhile, the probe **HCyXA-*β*Gal** showed a strong emission peak enhanced at 710 nm when excited at 680 nm (Fig. 1B), with a good linear relationship between fluorescent signals of **HCyXA-*β*Gal** and β-Gal (0–5 U/mL, correlation coefficient of $R^2 = 0.99822$; Fig. S1A in Supporting information). The limit of detection (LOD) was calculated to be 0.012 U/mL, which is comparable to relevant small fluorescent probe reported in the literatures [24,25,29].

To our delight, fluorescence enhanced very quickly in the initial 120 s when **HCyXA-*β*Gal** (10 μmol/L) was incubated with β-Gal (10 U/mL), and reached a maximum platform at 250 s (Fig. 1C, Figs. S1B and C in Supporting information). This response speed surpassed most of those reported probes for β-Gal (Table S1 in Supporting information), such as **DCM-*β*Gal** (35 min), **KSA01** (13 min), **CG** (15 min) and **Gal-Pro** (10 min) [23,25,29,30]. The steady-state kinetics of the enzymatic hydrolysis reaction was determined using fluorescence spectroscopy (Fig. S1D in Supporting information). By fitting curve using Michaelis-Menten equation, the K_m, V_{max}, k_{cat} and k_{cat}/K_m of reaction were calculated to be 68.37 μmol/L, 32.21 nmol L^{-1} s^{-1}, 104.59 s^{-1} and 1.53 L μmol^{-1} s^{-1}, respectively, indicating the high catalytic efficiency of **HCyXA-*β*Gal** to β-Gal. To demonstrate its applicability in bioimaging applications, the selectivity of **HCyXA-*β*Gal** towards β-Gal was also studied. As shown in Fig. 1D, **HCyXA-*β*Gal** exhibited high substrate specificity

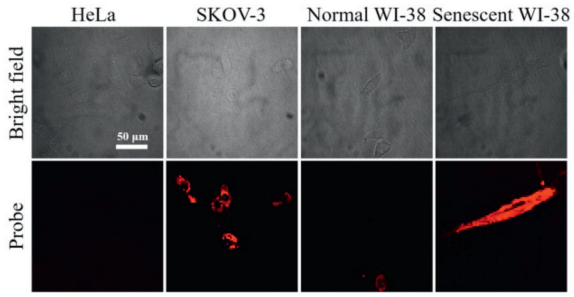

Fig. 2. Confocal images of HeLa cells, SKOV-3 cells, normal WI-38 cells and senescent WI-38 cells incubated with **HCyXA-βGal** (10 μmol/L) for 30 min. Ex/Em = 647/650−730 nm.

for β-Gal over common intracellular metabolites and other glycosidases. Considering the destructive effect of SA-β-Gal related lysosomal acidic environment [31,32], the stability of **HCyXA-βGal** and **HCyXA** were explored in different pH (Fig. S2 in Supporting information) and all showed good consistency for over 60 min. Furthermore, high resolution mass spectrometry (HRMS) verified that the changes in photophysical properties were induced by the β-Gal-mediated cleavage of **HCyXA-βGal** to **HCyXA** (Fig. S3 in Supporting information).

Motivated by the excellent responsive performance in the aspect of speed, selectivity and stability, **HCyXA-βGal** was then used for fluorescence imaging of endogenous β-Gal in living cells. As shown in Fig. 2, senescent WI-38 cells exhibited obviously enhanced fluorescence in the red channel while the fluorescent signal was barely observed for normal WI-38 cells after incubation with **HCyXA-βGal** (10 μmol/L) for 30 min. The significantly elongated cellular morphology and a commercial X-Gal staining assay were used to confirm that the increase of fluorescence in red channel was the result of SA-β-Gal expression (Fig. S4 in Supporting information). Similarly, OA-β-Gal in SKOV-3 (Fig. 2) also triggered the enhancement of the red channel. In contrast, no fluorescence was detected in HeLa cells where β-Gal expression is absent. The results above proved that the designed **HCyXA-βGal** has the capability of selective imaging for β-Gal in senescent cells and ovarian cancer cells, respectively. Subsequent cytotoxicity experiments indicated that the **HCyXA-βGal** is biocompatible and suitable for long term imaging studies (Fig. S5 in Supporting information).

Co-localization experiments were performed next to examine the organelle-targeting ability of probe **HCyXA-βGal**. As shown in Fig. 3, senescent WI-38 cells were incubated with commercially available organelle dyes (lysosome-targeting LysoTracker Green DND-26 and mitochondria-targeting MitoTracker Green FM) and then co-stained with **HCyXA-βGal** for 30 min. The Pearson's co-localization coefficients (R^2) were calculated to be 0.91 and 0.71 after overlapping the red channel from **HCyXA-βGal** with the green channel from LysoTracker Green DND-26 and MitoTracker Green FM, which demonstrated the SA-β-gal activity mainly occurred in the lysosomal compartments. As for the co-localization experiments of SKOV-3 cells (Fig. 3), the two values were 0.78 and 0.90, respectively, in accordance with the different location of OA-β-Gal [33]. These results demonstrate that **HCyXA-βGal** can specifically light-up by lysosomal SA-β-gal in senescent cells and mitochondrial OA-β-gal in SKOV-3 cells, while the poorer co-localization and weaker fluorescence intensity were evident in the absence of lysosome-targeting morpholinyl group [24,30]. The fluorescence imaging difference of enzymatic locations provides potential basis for differentiating senescent cells and ovarian cancer cells. It should be noted that the indistinctive difference between two co-localization coefficients of organelles may be caused by the diffusion of enzyme-activated fluorophores from POI in long incubation and imaging time.

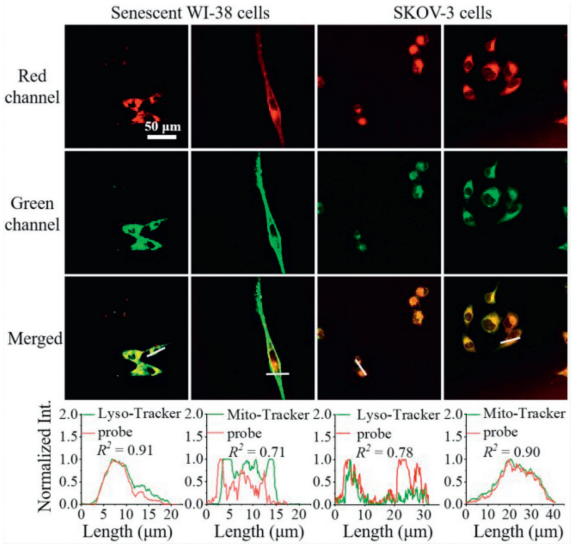

Fig. 3. Co-localization imaging of senescent WI-38 cells and SKOV-3 cells. The cells were incubated LysoTracker Green DND-26 or MitoTracker Green FM for 10 min and then incubated with **HCyXA-βGal** for 30 min. Green channel: Ex/Em = 488/500−550 nm. Red channel: Ex/Em = 647/650−730 nm.

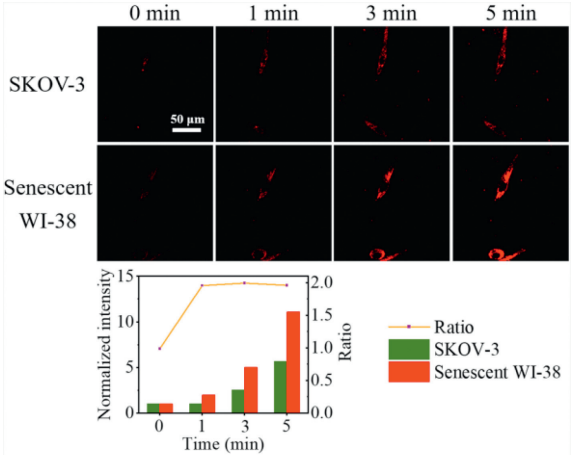

Fig. 4. Fast confocal fluorescence images and average normalized intensity of senescent WI-38 cells and SKOV-3 cells incubated with **HCyXA-βGal** at different time points. Red channel: Ex/Em = 647/650–730 nm.

Inspired by the fast-response performance of **HCyXA-βGal** towards β-Gal, the fast imaging experiments were designed for more precise identification of senescent cells and ovarian cancer cells. As shown in Fig. 4, real-time monitoring of β-Gal inside senescent WI-38 cells and SKOV-3 cells was carried out. The time-lapse images indicated that once **HCyXA-βGal** was incubated with cells, NIR fluorescence can be observed within 1 min and enhanced gradually with the increased incubation time (Video S1 in Supporting information). Interestingly, after the data processing through Image J software, we found the fluorescence intensity in senescent WI-38 cells was dramatically stronger than that in SKOV-3 cells. As a contrast, the long-time incubation and imaging experiments like Fig. 2 exhibited no discernible difference in the brightness of fluorescence during the imaging of senescent and ovarian cancer cells. This phenomenon indicated that the signal of time-dependent fluorescent intensity has the potential to be another dimension to differentiate senescent cells and ovarian cancer cells. Furthermore, dynamic monitoring Pearson's co-localization coeffi-

cients within a short time was examined to image senescent cells. As shown in Fig. S6 (Supporting information), the rapid and continuous increase of R^2 was observed in senescent WI-38 cells. Facilitated by the lysosome-targeting ability, the value of R^2 for senescent WI-38 cells rapidly reached 0.85 in five minutes. The results declared that imaging of senescent cells with probe **HCyXA-βGal** *via* tracking β-galactosidase is fast and accurate.

To conclude, we have reported a light-up NIR fluorescent probe **HCyXA-βGal** with bright NIR fluorescence response at short notice once incubated with cells containing β-Gal. By integrating the merits of organelle targetability and fast imaging capability, our probe design would find itself an effective tool and more accessible to cell differentiation between senescent cells and ovarian cancer cells *via* covering two dimensions of fluorescence signals: enzymatic location and time-dependent intensity. This can be a powerful complement to current state-of-the-art fluorescent probes of precise imaging in complex physiological conditions as well as early diagnosis.

Declaration of competing interest

The authors declare that they have no known competing financial interests or personal relationships that could have appeared to influence the work reported in this paper.

Acknowledgments

This work is supported by National Natural Science Foundation of China (Nos. 22122803 and 21788102) and the National Natural Science Foundation of Jiangsu Province (No. BK20220644).

Supplementary materials

Supplementary material associated with this article can be found, in the online version, at doi:10.1016/j.cclet.2023.108321.

References

[1] X. Huang, J. Song, B.C. Yung, et al., Chem. Soc. Rev. 44 (2018) 2873–2920.
[2] R. Liu, X. Wang, K. Aihara, L. Chen, Med. Res. Rev. 34 (2014) 455–478.
[3] J. Zhang, X. Chai, X.P. He, et al., Chem. Soc. Rev. 48 (2019) 683–722.
[4] G.P. Dimri, X. Lee, G. Basile, et al., Proc. Natl. Acad. Sci. U. S. A. 92 (1995) 9363–9367.
[5] B.Y. Lee, J.A. Han, J.S. Im, et al., Aging Cell 5 (2006) 187–195.
[6] B.G. Childs, M. Gluscevic, D.J. Baker, et al., Nat. Rev. Drug Discov. 16 (2017) 718–735.
[7] B. Lozono-Torres, A. Estepa-Fernández, M. Rovira, et al., Nat. Rev. Chem. 3 (2019) 426–441.
[8] A.P. Gomes, D. Ilter, V. Low, et al., Nature 585 (2020) 283–287.
[9] L. Connah, G. Angelovski, Org. Chem. Front. 7 (2020) 4121–4141.
[10] M. Perera, N. Papa, M. Roberts, et al., Eur. Urol. 77 (2020) 403–417.
[11] E.Edelman Saul, R.B. Guerra, M.Edelman Saul, et al., Nat. Cancer 1 (2020) 1140–1152.
[12] H. Singh, K. Tiwari, R. Tiwari, S.K. Pramanik, A. Das, Chem. Rev. 120 (2020) 4254–4255.
[13] Z. Yuan, J. Chen, Q. Zhou, et al., Chin. Chem. Lett. 32 (2021) 1803–1808.
[14] H. Yan, F. Huo, Y. Yue, J. Chao, C. Yin, J. Am. Chem. Soc. 143 (2021) 318–325.
[15] F. Debacq-Chainiaux, J.D. Erusalimsky, J. Campisi, O. Toussaint, Nat. Protoc. 4 (2009) 1798–1806.
[16] H.W. Lee, C.H. Heo, D. Sen, et al., Anal. Chem. 86 (2014) 10001–10005.
[17] B. Lozano-Torres, J.F. Blandez, I. Galiana, et al., Angew. Chem. Int. Ed. 59 (2020) 15152–15156.
[18] X. Li, W. Qiu, J. Li, et al., Chem. Sci. 11 (2020) 7292–7301.
[19] Y. Song, X. Li, D. Shi, et al., Chem. Sci. 13 (2022) 11738–11745.
[20] D. Asanuma, M. Sakabe, M. Kamiya, et al., Nat. Commun. 6 (2015) 6463.
[21] K. Gu, Y. Xu, H. Li, et al., J. Am. Chem. Soc. 138 (2016) 5334–5340.
[22] Z. Ding, C. Wang, M. Fan, et al., Chem. Commun. 56 (2020) 13579–13582.
[23] K. Gu, W. Qiu, Z. Guo, et al., Chem. Sci. 10 (2019) 398–405.
[24] X. Li, Y. Pan, H. Chen, et al., Anal. Chem. 92 (2020) 5772–5779.
[25] Y. Gao, Y. Hu, Q. Liu, et al., Angew. Chem. Int. Ed. 60 (2021) 10756–10765.
[26] X. Chai, H.H. Han, A.C. Sedgwick, et al., J. Am. Chem. Soc. 142 (2020) 18005–18013.
[27] Z. Wang, S. Chen, J.W. Lam, et al., J. Am. Chem. Soc. 135 (2013) 8238–8245.
[28] Y. Chen, C. Xue, J. Wang, et al., Chin. Chem. Lett. 33 (2021) 1637–1642.
[29] X. Kong, M. Li, B. Dong, et al., Anal. Chem. 91 (2019) 15591–15598.
[30] J. Zhang, C. Li, C. Dutta, et al., Anal. Chim. Acta 968 (2017) 97–104.
[31] J.L. Zhu, Z. Xu, Y. Yang, L. Xu, Chem. Commun. 55 (2019) 6629–6671.
[32] C. Jiang, L. Li, J. Jiang, et al., Chin. Chem. Lett. 31 (2020) 447–450.
[33] R. Long, C. Tang, Z. Yang, et al., J. Mater. Chem. C 8 (2020) 11860–11865.